Proceedings of ASME Turbo Expo 2021
Turbomachinery Technical Conference and Exposition
GT2021
June 7-11, 2021, Virtual, Online

GT2021-59429

INFLUENCE OF OPPOSING DILUTION JETS ON EFFUSION COOLING

M. Riley Creer and Karen A. Thole
The Pennsylvania State University
Department of Mechanical Engineering
University Park, PA 16802, USA

ABSTRACT

The gas turbine combustion process reaches gas temperatures that exceed the melting temperature of the combustor liner materials. Cooling the liner is critical to combustor durability and is often accomplished with double-walled liners that contain both impingement and effusion holes. The liner cooling is complicated with the interruption of the effusion cooling by large dilution jets that facilitate the combustion process. Given the presence of the dilution jets, it is important to understand the effect that the dilution jet has on the opposing wall in respect to the effusion film. This research includes measurements of the local static pressure distribution for a range of dilution jet momentum flux ratios to investigate the impact that the opposing dilution jet has on the effusion film. The interactions with the effusion cooling were also evaluated by measuring the overall cooling effectiveness across the panel.

Measurements show that the opposing dilution jets did impact the liner at dilution jet momentum flux ratios that were greater than 20. The impacts at high momentum flux ratios were indicated through increased local static pressures measured on the surface of the combustor liner. Furthermore, the dilution touchdown decreased the overall cooling effectiveness of the effusion cooling. Results also indicated that the opposing dilution jets changed position on the liner as the dilution jet momentum flux ratio changes.

INTRODUCTION

The durability of combustor liners is crucial to the safety of gas-turbine engines. In modern combustors, the temperature of the gases exceeds the melting temperature of materials used in turbines. As turbine inlet temperatures continue to rise, efficient cooling strategies increase in importance. An effective and commonly used cooling method for the combustor chamber is a double-walled liner comprised of an impingement shell and an effusion panel. The impingement plate produces impinging jets that cool the back side of the hot effusion plate while the effusion plate generates a cool film that protects the liner material from the combustion flows in the main gas path. In most combustor designs, the effusion film is disrupted by high momentum dilution jets used to mix the flow before entering the turbine. The interaction between dilution jets and the effusion film is complex; coolant is entrained by the dilution jet away from the wall that it is intended to cool. Flowfield measurements indicate that vortices wrap around the dilution jet much like a horseshoe vortex at the leading edge of a turbine airfoil. These vortices have been shown to decrease the effusion film effectiveness [1, 2].

Understanding the impact of dilution jets on effusion cooling is important to combustor liner durability not only in the vicinity of the dilution holes but also downstream of the dilution holes where effusion cooling is necessary. Given many combustor designs have opposing dilution jets in a staggered pattern, the effects of the opposing jets on the effusion cooling are of interest. When the momentum flux ratio is high, the dilution jets can impinge onto the opposing panel. The study reported in this paper was aimed at determining the effect that dilution jets have on the effusion cooling of the opposing combustor liner panel. The momentum flux ratio of the dilution jets was varied to understand the dilution jet impact on the effusion cooling for a non-reacting flow.

NOMENCLATURE

Bi	Biot number, $h_\infty t/k$
C	Holdeman parameter, $I_D^{1/2}(S_{p,D}/H_0)$
C_D	discharge coefficient
d	effusion hole diameter
D	dilution hole diameter
h	heat transfer coefficient

H	height between impingement and effusion walls
H_0	height of duct at dilution injection
I	momentum flux ratio, $\rho_c U_c^2 / \rho_\infty U_\infty^2$
k	thermal conductivity
L	effusion hole length
LD	lower dilution jets
M	blowing ratio $\rho_c U_c / \rho_\infty U_\infty$
P	static pressure
$S_{s,d}$	spanwise spacing of effusion holes
$S_{p,d}$	pitchwise spacing of effusion holes
$S_{p,D}$	pitchwise spacing of dilution holes
t	thickness of liner walls
T	temperature
UD	upper dilution jets
x,y,z	position measured from the center of the middle dilution hole
Greek	
α	effusion hole injection angle
Φ	overall cooling effectiveness, $(T_\infty - T_w)/(T_\infty - T_c)$
Subscripts	
c	coolant
D	dilution hole
ref	static pressure reference tap
w	wall
∞	mainstream
$\bar{(\ )}$	lateral average
i	interior

LITERATURE REVIEW

Many aspects of effusion cooling and dilution jets have been researched as gas-turbine engine temperatures have been pushed past material melting points. This section of the paper will provide a summary of relevant past studies on the general behavior of combustor liner effusion cooling, dilution jets and the interaction between the two.

Effusion cooling is implemented in combustor liners to develop a protective film of relatively cooler air that shields the combustor liner from the high-temperature main gas path temperatures. Although the cooling holes typically have short length-to-diameter ratios given the thin liner walls, angled effusion holes were found to cool the liner more effectively than normal holes as shown by Andrews et al. [3]. They also found that effusion holes injecting against the mainstream flow performed worse than effusion holes injecting aligned with the mainstream at high coolant flowrates.

Scrittore et al. [4] studied full-coverage, single-walled effusion cooling. For a multi-row effusion plate, they found that the effusion flow reached a fully developed flowfield downstream of the 15th row of cooling holes. The adiabatic film effectiveness had little variation from row to row once the flowfield became fully developed. Their study also determined that the velocity and turbulence profiles in the near wall layer scaled well with blowing ratio. Blowing ratio effects were investigated by Facchini et al. [5] by evaluating adiabatic film and overall cooling effectiveness of a single-wall effusion liner while increasing the blowing ratio. They discovered that adiabatic film effectiveness decreases with increasing blowing ratio while overall cooling effectiveness increases. Facchini et al. indicated the overall cooling effectiveness increase was due to in-hole convection and the adiabatic film effectiveness decrease was due to effusion jet liftoff.

In a gas-turbine combustor, dilution jets are often placed on opposite sides of the combustion chamber to increase mixing with the main gas path. Holdeman and Walker [6] examined single-side dilution jets in a heated crossflow and determined that the momentum flux ratio of the jet is an important parameter influencing jet penetration and mixing. Blomeyer et al. [7] investigated opposed dilution jets with a crossflow and determined there was an optimum momentum flux ratio for mixing. They also found that exceeding that optimum momentum flux ratio resulted in the opposing dilution jet impacting the combustor liner.

Other researchers have studied the interaction of dilution jets interrupting the effusion cooling film. The wake of a dilution jet in crossflow was studied by Fric and Roshko [8] and multiple vortical structures were observed. They found that multiple vortices form in the wake of the jet that entrain boundary layer fluid into the jet. A horseshoe vortex was also observed that wrapped around the leading edge of the jet. A slot film flow interrupted by a dilution jet was examined by Button [9]. They showed that the slot effectiveness was decreased by the jet. Martiny et al. [1] investigated a similar slot film with dilution jet and found that a vortex pair was formed by the jet that resulted in coolant separation and decreased effectiveness. A recirculation zone was found downstream of the dilution jet by Vakil and Thole [10]. These investigators analyzed a combustor liner with effusion cooling and dilution jets and found that a recirculation zone downstream of the dilution jet pulled warm fluid to the region directly downstream of the dilution hole despite the presence of cooling holes in that region. They attributed this warm flow to either horseshoe vortices wrapping around the jet or the reverse flow downstream of the jet. A similar liner with effusion cooling and dilution holes was investigated by Scrittore et al. [11] who found that as the dilution jet momentum flux ratio increased the downstream adiabatic film effectiveness decreased. The higher momentum flux dilution jets increased the turbulence which led to mixed out coolant flow thereby reducing the cooling.

Two studies [2,12] were conducted by Shrager et al. examining a double-wall combustor liner with a single-side dilution jet (no opposing dilution holes were included). The first study measured the overall cooling effectiveness [2] of three different effusion hole arrangements surrounding the dilution jets. These researchers found that outward facing holes yielded the best overall cooling effectiveness near the dilution holes. They also showed a wake of lower effectiveness downstream of the dilution jets. The companion paper [12] examined the flowfield of the same geometries. Downstream of the dilution jet, they found a stagnation region or a vortex depending on the effusion hole direction.

A study by Ahmed et al. [13] examined the difference between staggered and inline effusion cooling in a model combustor for both non-reacting and reacting flows. They determined that staggered effusion more effectively cooled the liner than inline effusion for both types of flows and that the overall cooling effectiveness increased as blowing ratio increased. Furthermore, this study showed that the swirling

combustion flow impinged on the combustor liner increasing the pressure and reducing the local overall cooling effectiveness.

While utilizing the same geometry as Shrager et al. [2,12], the current study is novel in that it evaluates the effect of double-sided, staggered dilution jets on the effusion liner cooling. Double-sided dilution jets were evaluated by Blomeyer et al. [5] but in the absence of any liner cooling. Although others have assessed the effect of single-sided dilution on film cooling, no one has analyzed how double-sided dilution influences the effusion cooling of a combustor liner. Furthermore, by analyzing both the local static pressure and overall cooling effectiveness, the interaction between dilution jets and effusion cooling is clearly demonstrated.

EXPERIMENTAL METHODS

Two types of measurements were used to evaluate the impact an opposing dilution jet has on the combustor liner effusion cooling: static pressure and overall cooling effectiveness. The static pressure distribution across the liner was measured to demonstrate how the dilution jets interact with the liner for a variety of flow conditions. Additionally, to quantify how the dilution jet interaction affects the cooling of the liner, the overall cooling effectiveness was measured in a matched Biot number test. Past research by Williams et al. [14] and Mensch and Thole [15] demonstrated that matching Biot number and the ratio of external and internal heat transfer coefficients, h_∞/h_i, results in data that can be compared to the engine. Note that for the static pressure measurements, no effusion holes were present in the panel, which allowed for a high density of static pressure measurements.

A benchtop rig was constructed to simulate a combustor sector that included an abundance of instrumentation as shown in Figure 1. Note that no combustion was present in this experiment and air was used as the working fluid. As shown in Figure 1, the rig had three flow paths, each controlled by a separate mass flow controller. For the measurements of overall cooling effectiveness, the mainstream flow passed through a heater before entering the test rig to provide a temperature differential between the main gas path and the cooling flows.

The effusion holes and lower dilution (LD) jets are fed from the same air source that enters a plenum beneath the combustor liner panel, as shown in Figure 1. A baffle plate and screen condition the flow at the entrance of the plenum. The upper dilution (UD) jet flow is supplied by a separate air source to a plenum on top of the rig and is normalized by a baffle plate and screen. No effusion cooling was present on the top wall; only the UD holes in a staggered pattern were present.

Thermocouples were used to measure the temperature of the three flows in each plenum, which were set to be matched. Three thermocouples were positioned near the exit of the mainstream plenum and averaged together to determine the mainstream temperature. The typical temperature difference between the main gas path and the cooling and dilution holes was nominally 35 °C. The temperature of the UD flow, LD flow, and the bottom effusion flow was maintained to within 0.5 °C. A static pressure tap located after the liner contraction was used to measure the mainstream static pressure. The bottom coolant plenum contains three thermocouples and a static pressure tap that measure the temperature and pressure of both the effusion cooling and LD flows. Similarly, the temperature and pressure of the UD flow are measured with two thermocouples and a static pressure tap located in the top coolant plenum. Insulation was used to minimize heat transfer between the rig and the surroundings.

As was discussed, two panels were used for this study on the bottom wall, as shown in Figure 2. The first panel was a single wall that included the dilution holes and pressure taps for the static pressure measurements, but due to the large number

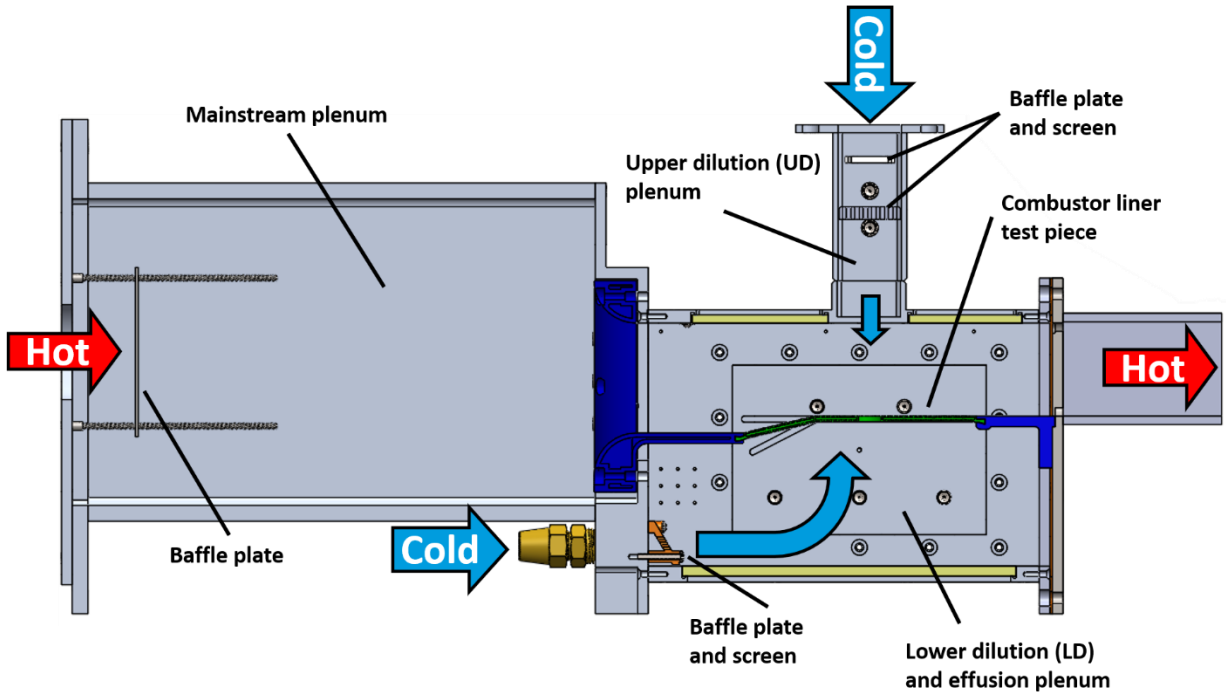

Figure 1 Illustration of the rig showing the mainstream flowpath and two coolant flowpaths

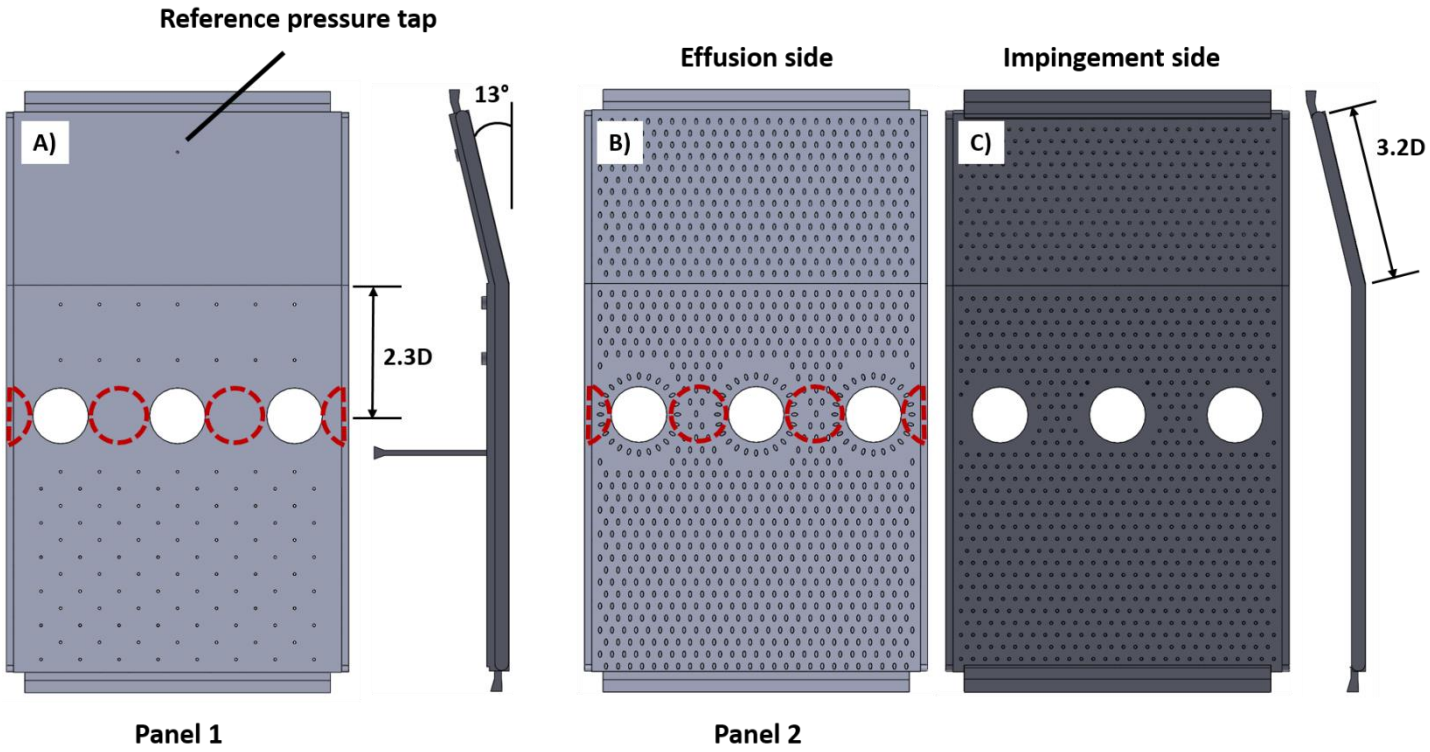

Figure 2 Combustor liner panels used for this study including a) the single-wall pressure tap panel; b) top side of double-wall effusion panel and c) bottom side of double-wall panel. Note dashed red circles are diffusion holes on the opposing wall.

of pressure taps did not include any film-cooling holes. The second panel was a double-walled panel with identical dilution holes as the first panel, but also included an effusion hole pattern that was the same as that used by Shrager et al. [2, 12]. Both panels included a sloped leading edge that was angled down 13° as shown in Figure 2, which differed from that of Shrager et al. who used a flat approaching wall. The dilution hole diameter on both panels was D = 13.9mm and the pitchwise spacing was 2.1D. Surrounding the dilution holes, as shown in Figure 2b, are inward facing effusion holes that are spaced 0.69D from the dilution hole center. The diameter of the effusion and impingement holes was d = 0.61 mm and the hole and spacing specifications are shown in Figure 3. The impingement hole spacing pattern was offset from the effusion hole pattern by 1.8d.

Opposite the bottom liner panel, the UD holes were machined to have the same diameter as those on the bottom wall panel. These UD holes were staggered from the LD holes on the panel and appear in Figure 2 as dashed red circles.

Static pressure measurements and overall cooling effectiveness measurements were recorded as momentum flux ratio of the dilution hole jets was varied from I_D = 10, 20, 30, and 40. The momentum flux ratio for the dilution jets was calculated using the inlet mainstream mass flow rate measured upstream of any injection. The mainstream mass flow rate increased down the panel due to the effusion cooling by 9% at I_D = 10 and 15% at I_D = 40. Downstream of dilution injection, the combined UD and LD jets increased the mainstream flow rate by 63% at I_D = 10 and 127% at I_D = 40. Furthermore, tests were also performed with either UD or LD jets turned off to see the effect of each jet individually on the combustor liner panel.

Static Pressure Measurements

A combustor panel outfitted with an array of pressure taps was used to measure the static pressure distribution for the four momentum flux ratios stated earlier. The test article used was Panel 1, shown in Figure 2a, and it included 3 dilution holes of the same diameter listed above but no impingement or effusion holes. A bi-directional differential pressure scanner was used to measure 96 static pressure taps on the panel. The pressure differential was measured relative to an upstream reference pressure tap, labeled in Figure 2a, and nondimensionalized, as shown in Equation (1), by the pressure differential between a mainstream static pressure tap and the same panel reference tap.

$$\Delta P = \frac{P_{ref} - P}{P_{\infty} - P_{ref}} \qquad (1)$$

The definition of this equation resulted in high ΔP values for high local static pressure readings. Once steady pressure measurements were noted, the average pressure differential at each pressure tap was calculated from 1100 data points collected over four minutes. The calibration of the pressure scanner was validated using a manometer and determined to be within specification.

Overall Cooling Effectiveness Measurements

The overall cooling effectiveness measurements were collected using the double-walled combustor liner, labeled Panel 2 in Figures 2b and 2c; further details of Panel 2 are shown in Figure 3 and Table 1. Typical of a double-walled design, a pattern of impingement holes covers the cold side of the panel which feed a pattern of angled effusion holes that

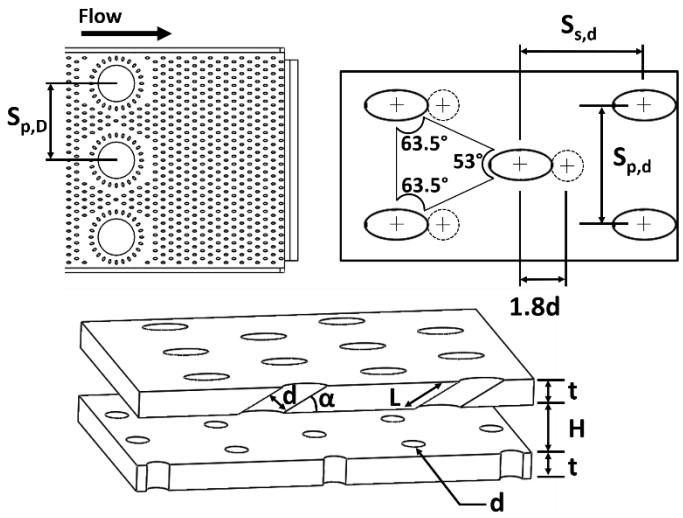

Figure 3 Schematic detailing the geometry used on Panel 2. This geometry was created by scaling down the geometry used by Shrager et al. [2,12].

covers the hot side, seen in Figure 2c and Figure 2b respectively.

The geometry used for the double-walled liner is a scaled version of that used by Shrager et al. [2,12], although Shrager et al. did not have a leading edge that was angled. Panel 2 was 3D printed using a high temperature resin with a measured thermal conductivity of k = 0.195 W/m-K.

TABLE 1. PANEL GEOMETRY PARAMETERS

Parameter	Value
D	13.9 mm
d	0.61 mm
α	30°
L/d	2.8
t/d	1.4
H/d	2.6
$S_{s,d}/d$	4.9
$S_{p,d}/d$	4.9
$S_{p,D}/D$	2.1

To ensure the data is relevant to gas turbine combustors, the non-dimensional parameters Biot number, Bi, and heat transfer coefficient ratio, h_∞/h_i, were matched as closely as possible to that of a typical combustor [14, 15]. The exterior heat transfer coefficient, h_∞, was calculated using a local turbulent correlation for Nusselt number calculated at the middle and end of the panel and averaged together. The interior heat transfer coefficient was estimated using an average Nusselt number correlation for staggered impingement jets with vent holes from Hollworth and Dagan [16] for each jet momentum flux ratio. These values are listed in Table 2 for the different momentum flux ratio conditions.

The overall cooling effectiveness is calculated using Equation (2) with T_∞ as the mainstream temperature, T_c as the bottom coolant temperature and T_w as the panel wall temperature.

$$\Phi = \frac{T_\infty - T_w}{T_\infty - T_c} \qquad (2)$$

Infrared thermography was used to measure the steady-state panel wall temperature. An infrared camera, calibrated *in situ*, captured 10 images one second apart that were averaged together. To calibrate the camera, four thermocouples were attached to the panel with thermally conductive epoxy. The infrared camera was placed above the test rig looking upstream through the downstream Zinc Selenide window. Additionally, to eliminate any reflections, the camera was angled. The panel was not painted since it has a high emissivity of ε = 0.94, which is desirable for accurate temperature measurements.

TABLE 2. ENGINE RELEVANT PARAMETERS

Parameter	Values		Engine Values [2,12]
I_D	10, 20, 30, 40		33
k [W/m-K]	0.195		22
$Bi = h_\infty t/k$	0.15		~ 0.02
h_∞/h_i	$I_D = 10$	0.019	
	$I_D = 20$	0.018	~ 0.15
	$I_D = 30$	0.017	
	$I_D = 40$	0.016	

Because the LD holes are fed from the same air supply as the effusion cooling air, the mass flow through the dilution holes was calculated using the pressure difference in the plenum and the main flow path and an assumed discharge coefficient of $C_D = 1$. It was found that 80% of the bottom cooling flow went through the dilution holes while the other 20% flowed through the effusion holes for the $I_D = 40$ case, as shown in Table 3. The dilution flow percentage was constant for I_D = 30, 20 but decreased to 78% at $I_D = 10$. The Holdeman parameter [17], C, for each flow condition is also shown in Table 3 for reference.

TABLE 3. SUMMARY OF FLOW CONDITIONS

I_D	C	Flow Split		Mainstream flow addition	
		Effusion	LD	Effusion	UD and LD
10	1.7	22%	78%	9%	63%
20	2.3	20%	80%	11%	90%
30	2.9	20%	80%	13%	112%
40	3.3	20%	80%	15%	127%

UNCERTAINTY ANALYSIS

An analysis was performed to quantify the uncertainty of the momentum flux ratio measurements, the static pressure distribution and the overall cooling effectiveness measurements. The partial derivative method developed by Moffat [18] was used for these estimates. The uncertainty of the overall cooling effectiveness measurements was highest at 7% for Φ = 0.69 and lowest at 5.6% for Φ = 0.97. This uncertainty was dictated by the calibration thermocouples. Average overall cooling effectiveness uncertainty was below 0.4% for all tests. Typical uncertainties for the static pressure measurements of the combined dilution flow condition ranged from 58% - 82% for ΔP = -5.1 to ΔP = 5.3. The relative uncertainty of the

momentum flux ratio was calculated to be less than 1% for all momentum flux ratios.

PRESSURE MEASUREMENT RESULTS

The static pressure distribution was recorded for a variety of flow conditions. Presented first in Figure 4 are the low momentum flux ratio I_D = 10 results for three different flow conditions: combined UD and LD, LD only, and UD only. The combined dilution case and LD case, presented in Figures 4a and 4b respectively, show low static pressure regions behind the dilution holes, at approximately x/D ~ 1, indicating that the LD jets have an influence on the static pressure distribution. These low static pressure regions are formed by a recirculation vortex downstream of the dilution jet injection that leads to coolant separation. Flowfield results collected by Shrager et al. [12] for a similar combustor liner showed a vortex downstream of the dilution jets that is caused by shear. Similar vortical structures were detected by Fric and Roshko [8] and Vakil and Thole [10]. This vortex entrains the effusion flow into the dilution jet and results in a low-pressure region downstream of dilution injection.

The UD case shown in Figure 4c, when compared with both the combined dilution and LD flow cases, shows nearly uniform static pressure on the combustor liner. In the UD contour, the absence of the LD jets eliminates the separation region behind the LD jets and thereby the local decrease in static pressure in that area.

The static pressure distribution is quite different at a high momentum flux ratio of I_D = 40 as presented in Figures 5. The combined dilution case and UD case, shown in Figure 5a and 5c respectively, exhibit two high static pressure regions downstream of the dilution holes at approximately x/D ~1.5.

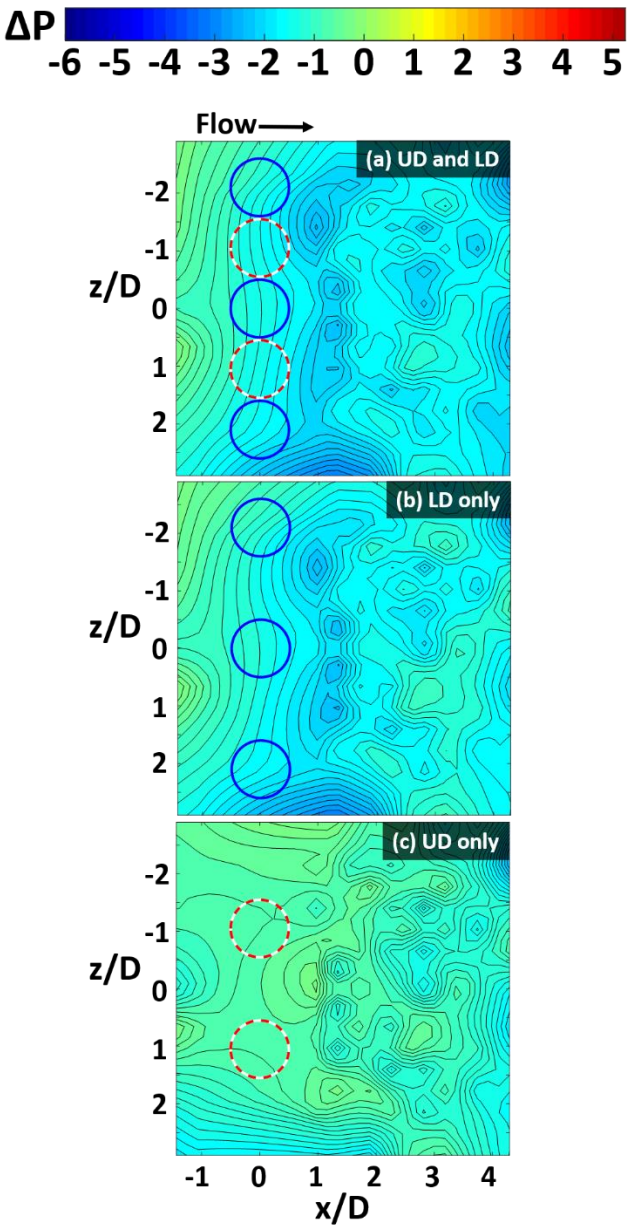

Figure 4 Static pressure contours of momentum flux ratio I_D = 10 for three flow conditions: a) combined UD and LD, b) LD only, and c) UD only.

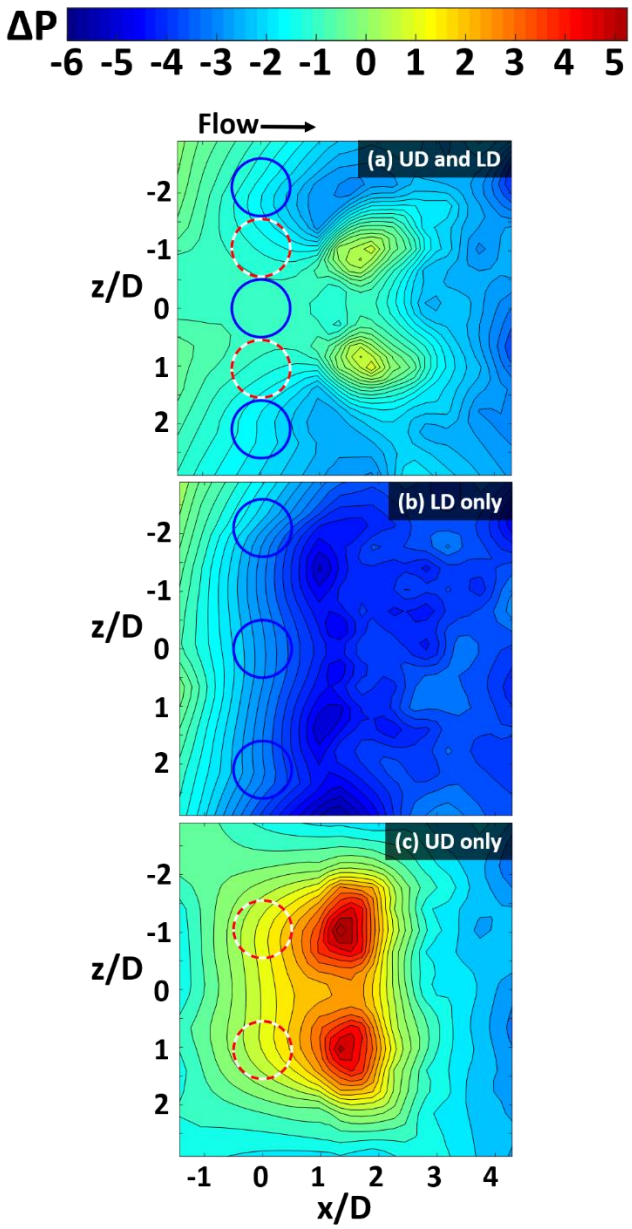

Figure 5 Static pressure contours of momentum flux ratio I_D = 40 for three flow conditions: a) combined UD and LD, b) LD only and c) UD only.

These high static pressure regions are caused by the high momentum UD jets impacting the opposite wall of the combustor panel. The high pressure UD touchdown region in the combined dilution contour seen in Figure 5a is smaller than the UD only contour in Figure 5c due to the interactions of the staggered UD and LD jets. As demonstrated by Scrittore [19], in the combined dilution flow case, the staggered UD jets and LD jets interact, create a shear layer. This shear layer between the opposing jets increases the local turbulence resulting in a high mixing region that results in a smaller UD touchdown area observed in the combined dilution contour in Figure 5a when compared to the UD only contour in Figure 5c.

Comparing the LD cases from momentum flux ratios of I_D = 10 and I_D = 40, seen in Figures 4b and 5b, a decrease in static pressure across the liner is detected as momentum flux ratio is increased. The additional dilution jet massflow for the I_D = 40 case compared with the I_D = 10 case serves to increase the velocities and decrease the static pressures along the liner. This general static pressure decrease due to the additional massflow is also observed around the edges of the combined dilution and UD only contours in Figures 5a and 5c but the UD touchdown effect is more prominent and dominates the static pressure distribution in those flow cases.

Static pressure contours of all four momentum flux ratios with the combined UD and LD flow condition are seen in Figure 6. The UD touchdown is clearly visible at momentum flux ratio I_D = 30 and 40, as shown in Figure 6c and 6d. Results also show that as momentum flux ratio increases from 30 to 40, the high-pressure touchdown area shifts farther upstream and increases in magnitude. These relative changes are due to the jet penetration being further into the mainstream which is determined by the momentum flux ratio of the jet. At the lower momentum flux ratio of I_D = 20 presented in Figure 6b, a pressure peak caused by UD touchdown is still visible though much weaker when compared to the I_D = 30 and I_D = 40 cases. Figure 6 demonstrates that the UD jets make contact with the combustor liner causing a local static pressure spike at momentum flux ratios above I_D = 20.

Spanwise line plots reveal more about this UD touchdown at different momentum flux ratios. Figure 7 presents how ΔP changes across the panel at different streamwise x/D locations across the combustor panel for the four momentum flux ratios tested. The I_D = 10 case, presented in Figure 7a, shows little pressure variation down the panel. The pressure peak caused by UD touchdown effect is slightly visible at momentum flux ratio of I_D = 20, shown in Figure 7b, at x/D=2.5. As momentum flux ratio increases to I_D = 30 in Figure 7c, the UD touchdown is observed at x/D=2 and x/D=2.5, with the slightly higher static pressure recorded at x/D=2.5. The I_D = 40 case, in Figure 7d, shows a static pressure peak at the same x/D locations of x/D=2 and x/D = 2.5, but with the former being higher. Comparing the ΔP line plots from these different momentum flux ratios in Figure 7 confirms that the static pressure increase caused by the UD touchdown increases with momentum flux ratio. These plots also verify that the touchdown area is moving upstream as momentum flux ratio increases.

The impact of these local static pressure measurements due to the dilution jets was calculated in terms of an expected local effusion blowing ratio using the static pressure measurements

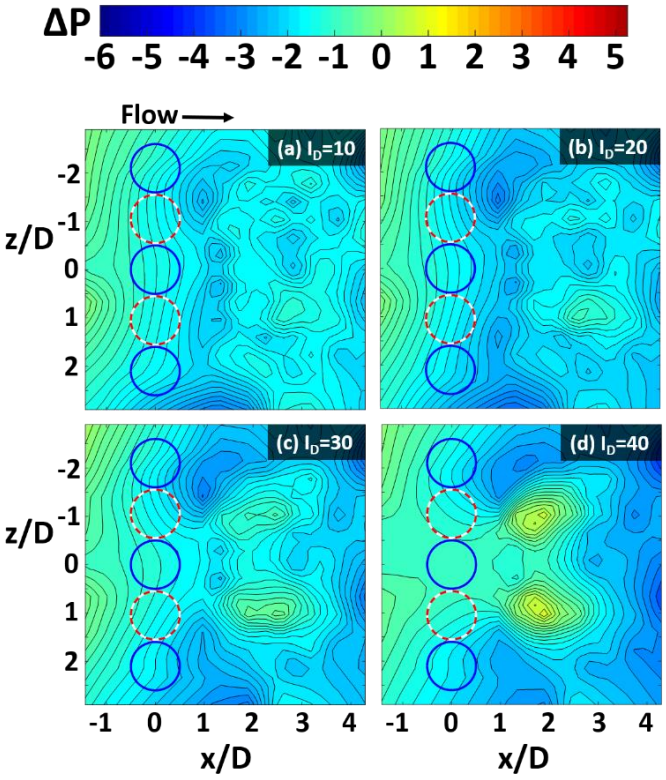

Figure 6 Static pressure contours of combined UD and LD case for all four momentum flux ratios: a) I_D = 10, b) I_D = 20, c) I_D = 30, and d) I_D = 40.

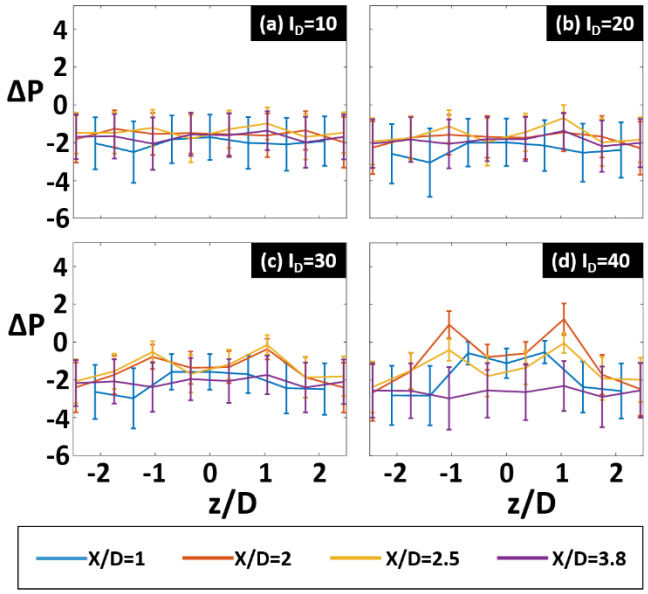

Figure 7 Spanwise static pressure plots at different x/D locations for four momentum flux ratios: a) I_D = 10, b) I_D = 20, c) I_D = 30, and d) I_D = 40

for two flow conditions at I_D = 40. The calculated local blowing ratio results, shown in Figure 8, assumed a discharge coefficient of C_D = 0.7. The UD case was not included because the blowing ratio calculations used the LD plenum pressure to predict

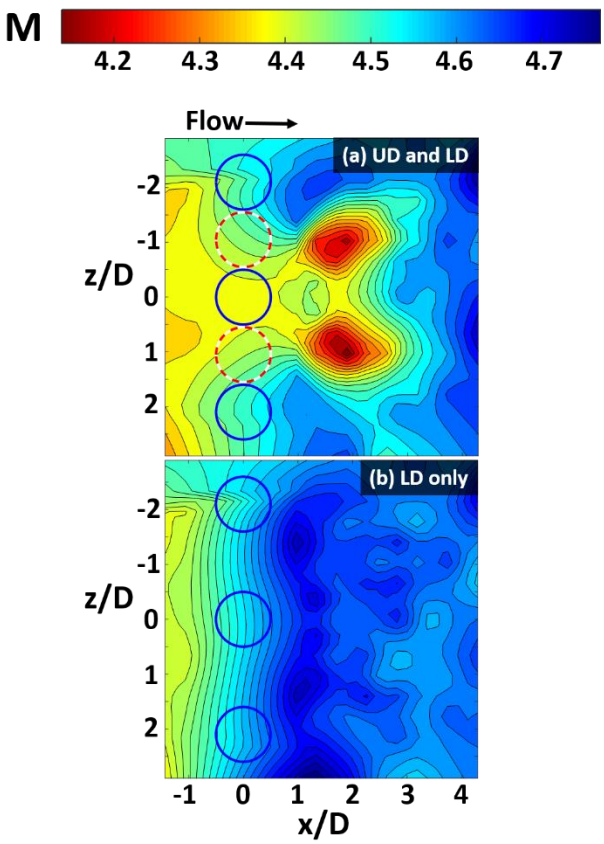

Figure 8 Blowing ratio contours showing the impact dilution jets have on effusion blowing ratio.

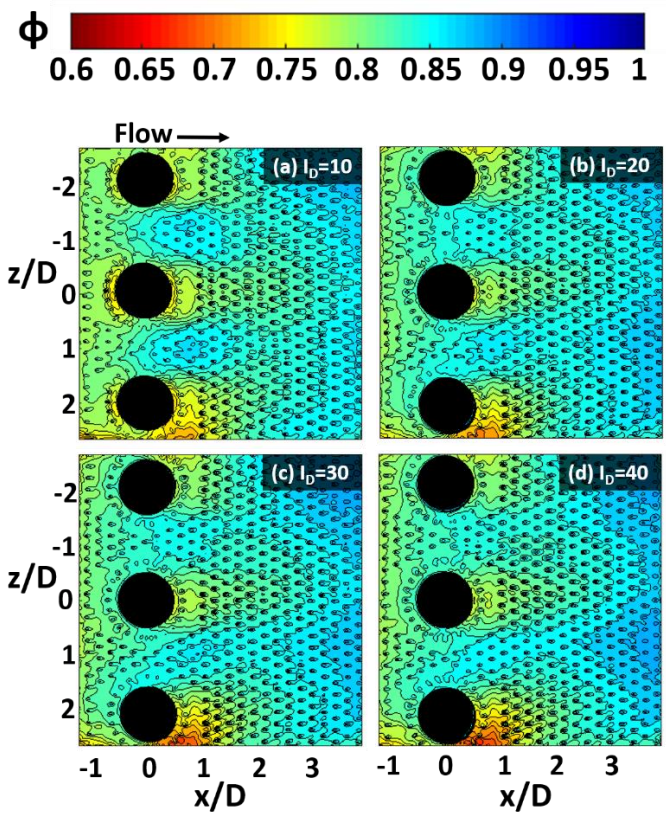

Figure 9 Overall cooling effectiveness contours showing the effect of LD jets on the downstream effusion

effusion velocity and this plenum was blocked off for the UD only flow condition. The combined UD and LD case, presented in Figure 8a, show a predicted decrease in the local blowing ratio in the UD touchdown area relative to the rest of the combustor liner. The local static pressure increase on the combustor liner surface caused by the UD touchdown leads to a lower velocity through the effusion holes and therefore a decreased local blowing ratio. The LD only results seen in Figure 8b predict an increase in blowing ratio in the dilution wake area. This blowing ratio increase is due to the decrease in static pressure downstream of dilution injection, displayed in Figure 5b, that begets increased effusion velocity.

OVERALL COOLING EFFECTIVENESS MEASUREMENTS

Infrared thermography measurements collected using Panel 2, the double-wall effusion panel displayed in Figure 2b and 2c, were used to calculate the overall cooling effectiveness for different flow conditions. Displayed first are overall cooling effectiveness contours with only LD and effusion flow, shown in Figure 9. A region of reduced overall cooling effectiveness is seen directly downstream of the LD jets at all four momentum flux ratios. These areas of reduced effectiveness in the dilution hole wake also appear in the results collected by Shrager et al. [2] using a similar panel. The static pressure measurements for the LD only flow condition, seen in Figures 4b and 5b, showed low static pressure zones in this same area. As discussed earlier, the LD jets block the mainstream flow resulting in a flow separated region. Reduced mainstream flow in this area results in higher momentum flow through the effusion holes leading to coolant separation and lower overall cooling effectiveness. The wake vortices also contribute to the lower overall cooling effectiveness by drawing effusion cooling air away from the liner. The two outer wake regions curl inward slightly and merge with the center wake due to sidewall effects of the test facility.

Examining the results with only the UD jets in Figure 10 clearly shows the UD touchdown that was observed in the static pressure measurements. At momentum flux ratio of I_D = 10, seen in Figure 10a, the overall cooling effectiveness increases steadily down the liner similar to the film cooling studies of Scrittore [4] and Facchini [5], suggesting that the UD jets have no effect on the liner at this momentum flux ratio. At higher momentum flux ratios of I_D = 20, I_D = 30, and I_D = 40; however, the UD touchdown has an increasing detrimental effect to the overall cooling effectiveness. The UD jets splash down on the combustor liner and cause a local reduction in overall cooling effectiveness, seen in Figures 10b-d. This region of reduced effectiveness corresponds with the increased static pressure zones seen in Figures 6b-6d. The local increased static pressure caused by the UD jets making contact with the combustor liner reduces the local effusion flow and thereby the overall cooling effectiveness. Similar to the static pressure results in Figure 6c and 6d, the UD touchdown moves upstream as the momentum flux ratio is increased.

Double-sided dilution impacts the effusion in a complex way as shown by the effectiveness contours with both UD and LD jets in Figure 11. At low momentum flux ratios of I_D = 10

and I_D = 20 the combined dilution data shown in Figures 11a and 11b show closely matched contour patterns and levels with the LD case in Figures 9a and 9b. This confirms that, at low momentum flux ratios, UD has very little impact on the effusion downstream of the dilution holes. At higher momentum flux ratios of I_D = 30 and I_D = 40, the double-sided dilution contours in Figures 11c and 11d show areas of reduced effectiveness that correspond to the UD jet splashdown. Not surprisingly, the location of the UD jet splashdown changes between single sided dilution and double-sided dilution when comparing Figures 10c-d and Figure 11c-d respectively. As discussed in the static pressure results, the UD splashdown changes location between the UD flow condition and the combined UD and LD flow condition due to the shear layer that develops with the addition of the LD jets. Additionally, the impact of the UD jets on overall cooling effectiveness is clearly visible on the -z side of the liner while only faintly visible on the +z side in Figures 11c and 11d. This is likely due to a misalignment of the staggered jets that results in increased mixing of the +z UD jet with the LD jets.

Demonstrating UD splashdown at momentum flux ratios as low as I_D = 30 contradicts past studies. The optimum momentum flux ratio correlation developed by Blomeyer et al. [7] was used to predict the optimum momentum flux ratio for this experimental setup as I_D = 84, meaning that UD splashdown should not occur at momentum flux ratios below I_D = 84. This correlation takes into account the ratio of dilution hole pitch to dilution hole diameter, $S_{p,D}/D$, and the ratio of duct height to dilution hole diameter, H_0/D. Blomeyer et al. studied a range of pitch-to-diameter ratios of $S_{p,D}/D$ = 2-6 and height-to-diameter ratios of H_0/D = 5-12.5. The parameters of the current study are similar at $S_{p,D}/D$ = 2.1 and H_0/D = 4. However, that correlation was developed by measuring the temperature of the mainstream gas path not the liner itself, so the current study provides a more complete understanding of the dilution jet effect on the combustor liner. Similarly, Holdeman [17] concluded that over-penetration of the dilution jets occurs when values of the Holdeman parameter are twice the optimum value, which he lists as C = 5 for the staggered dilution configuration. The Holdeman parameter accounts for the momentum flux ratio of the dilution jet, I_D, as well as the ratio of dilution hole pitch to duct height, $S_{p,D}/H_0$. While Holdeman tested geometries with a range of $S_{p,D}/H_0$ = 0.25-1, only a pitch-to-height ratio of $S_{p,D}/H_0$ =0.52 was used for the current study. As shown in Table 3, the I_D = 40 condition had the largest Holdeman parameter of the study at C = 3.3, below both the optimum of C = 5 and Holdeman's threshold for over-penetration of C = 10. By measuring the liner temperature and static pressure fields to create overall cooling effectiveness and static pressure distributions, it is clear that double sided dilution impacts the effusion cooling of the liner through a splashdown effect well below the optimum mixing momentum flux ratio defined by Blomeyer et al and Holdeman.

The UD impact on effusion was quantified by computing the lateral average of the overall cooling effectiveness. Compared in Figure 12 are the overall cooling effectiveness lateral averages of seven different test conditions including one from Shrager et al. [2]. The combined dilution cases are shown

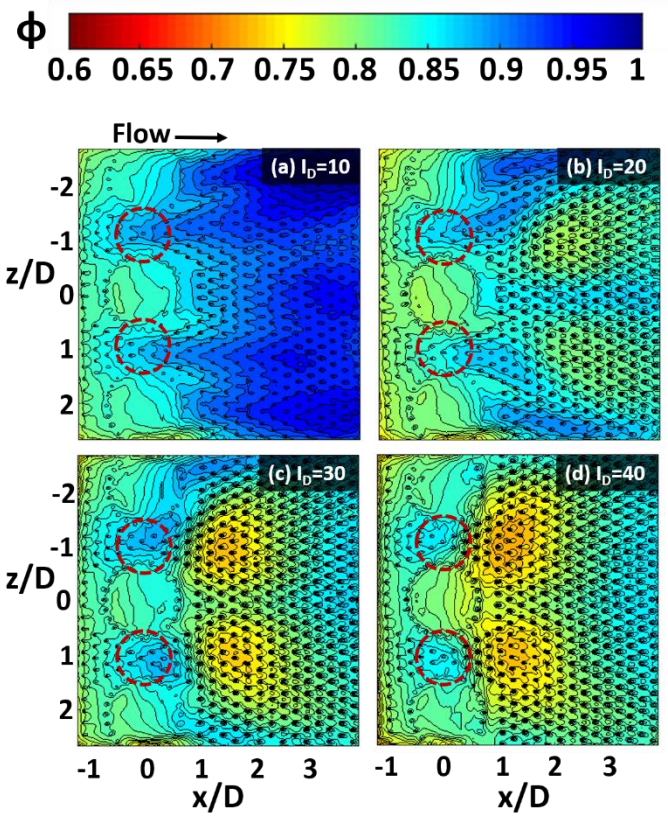

Figure 10 Overall cooling effectiveness contours showing the effect of UD jets

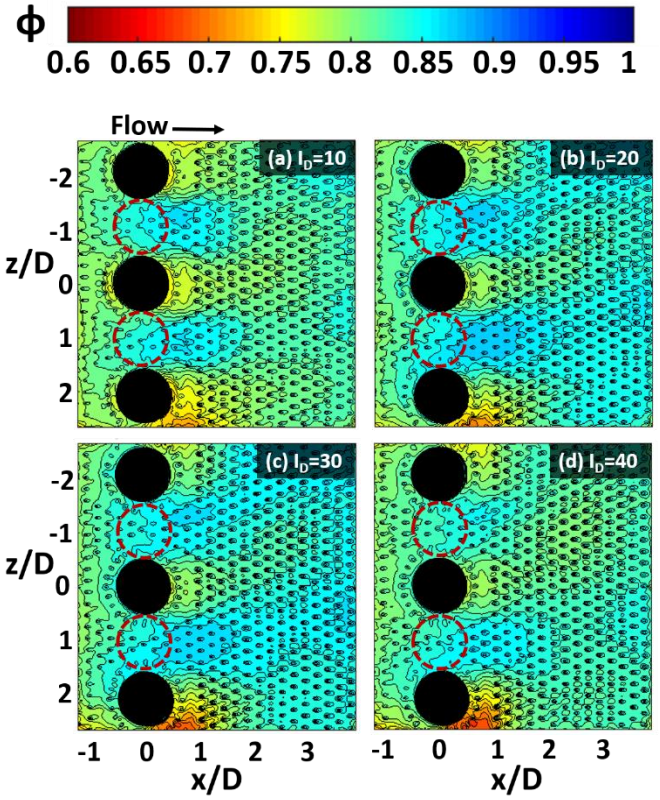

Figure 11 Contours showing the UD and LD jets impact on the effusion cooling

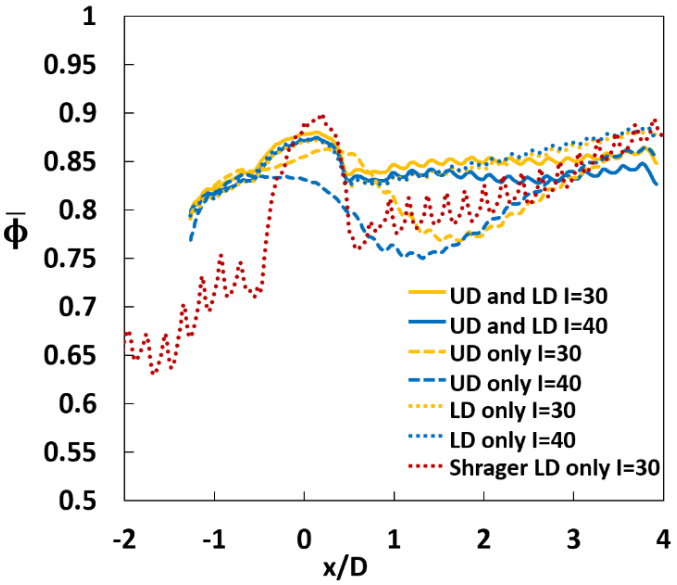

Figure 12 Line plots of lateral average of overall cooling effectiveness for all test conditions of momentum flux ratios I_D =30 and 40. Also included is data from Shrager et al. [2]

with solid lines while the UD and LD cases are shown with dashed and dotted lines, respectively.

Figure 12 shows that the UD touchdown effect results in a significant decrease in effectiveness values for both momentum flux ratios of I_D = 30 and I_D = 40. As shown earlier, the touchdown effected area shifts upstream as momentum flux ratio is increased. These decreases in average overall cooling effectiveness are also present in the combined UD and LD cases; however, the decrease in average effectiveness occurs farther downstream of the dilution holes than the UD only case. The average overall cooling effectiveness decreases rather than steadily increasing as it does in the LD only results, demonstrating the reduced cooling for the UD jet case resulting from the high turbulence levels. Furthermore, the average overall cooling effectiveness results of the combined UD and LD tests confirm the conclusion that the UD touchdown area moves upstream and increases in magnitude with increasing momentum flux ratio.

In comparing to Shrager et al. [2], the LD only results of the current study indicate higher average overall cooling effectiveness. It is important to note that there are two differences between the current study and the Shrager et al. study: the current study has an increased number of effusion holes upstream of the dilution injection and an angled approach surface whereas the Shrager et al. study used a flat test panel. These differences result in higher average effectiveness than the results from Shrager et al.

CONCLUSIONS

Two combustor liners with double-sided, staggered dilution jets were evaluated for static pressure distribution and overall cooling effectiveness. The first panel was instrumented with an array of static pressure taps to record the effect of dilution jet momentum flux ratio on the combustor liner static pressure distribution. The second panel featured double-walled effusion cooling and demonstrated how the dilution jet momentum flux ratio impacted the overall cooling effectiveness.

The static pressure distributions showed that both upper and lower dilution jets affect the downstream combustor liner pressure distribution. Low static pressure pockets formed directly downstream of the LD jets with the UD jets turned off. It was found that as the dilution jet momentum flux ratio increased the static pressure in this area decreased. The UD jets caused a local static pressure increase by splashing down on the combustor liner at momentum flux ratios above I_D = 20. As the momentum flux ratio increased for these cases with the splashdown, this high static pressure zone moved upstream towards the dilution holes. The double-sided dilution tests revealed that at low momentum flux ratios, the LD jets dominate the static pressure distribution by causing low pressure pockets downstream of the dilution holes. At high momentum flux ratios, the opposite is true, and the UD jets had a larger influence on the liner pressure by causing the high static pressure touchdown zones.

Consistent with the changes in the local static pressures, the UD and LD jets also impacted the overall cooling effectiveness measurements. Single-sided LD flow caused low effectiveness wakes downstream of the LD holes. These low effectiveness wakes were present at all momentum flux ratios. The UD touchdown effect was visible in single-sided UD tests at momentum flux ratios above I_D = 20. With double-sided dilution, the low effectiveness wakes dominate the combustor liner effusion cooling at low momentum flux ratios. As momentum flux ratio increases above I_D = 30, the UD jet touchdown reduces local overall cooling effectiveness downstream of the dilution holes. The UD touchdown effect is less prominent with double-sided dilution flow, suggesting that the interaction of double-sided dilution jets is an important consideration.

This work highlights the need to consider the dilution jets impact on liner cooling during combustor design. The goal of mixing out combustor flow needs to be balanced with the dilution jet influence on effusion. It also uncovers questions to be addressed in future work including how different effusion or dilution hole patterns might mitigate the impact of dilution jet touchdown to cooling effectiveness.

REFERENCES

1. Martiny, M., Schulz, A., Wittig, S., and Dilzer, M., 1997, “Influence of a Mixing-Jet on Film Cooling,” 97-GT-247.
2. Shrager, A. C., Thole, K. A., and Mongillo, D., 2018, "Effects of Effusion Cooling Pattern Near the Dilution Hole for a Double-Walled Combustor Liner: Part 1 — Overall Effectiveness Measurements." *ASME J. Eng. Gas Turbines Power*, **141**(1), pp. 011022.
3. Andrews, G. E., Khalifa, I. M., Asere, A. A., and Bazdidi-Tehrani, F., “Full Coverage Effusion Film Cooling with Inclined Holes,” 95-GT-274.
4. Scrittore, J. J., Thole, K. A., and Burd, S. W., 2007, “Investigation of Velocity Profiles for Effusion Cooling of a Combustor Liner,” *ASME J. Turbomach.*, **129**, pp. 518–526.

5. Facchini, B., Tarchi, L., Toni, L., and Ceccherini, A., 2010, "Adiabatic and Overall Effectiveness Measurements of an Effusion Cooling Array for Turbine Endwall Application," *ASME J. Turbomach.*, **132**(4), pp. 041008.
6. Holdeman, J. D., and Walker, R. E., 1977, "Mixing of a Row of Jets with a Confined Crossflow." *AIAA J*., **15**(2), pp. 243–249.
7. Blomeyer, Malte M., et al., 1996, "Optimum Mixing for a Two-Sided Injection From Opposing Rows of Staggered Jets Into a Confined Crossflow." 96-GT-453.
8. Fric, T. F., and A. Roshko, 1994, "Vortical Structure in the Wake of a Transverse Jet." *J. of Fluid Mechanics*, **279**, pp. 1–47.
9. Button, B. L., 1984, "Effectiveness Measurements for a Cooling Film Disrupted by a Single Jet," *Int. Comm. Heat Mass Transf*., **11**(6), pp. 505–516.
10. Vakil, S. S., and Thole, K. A., 2005, "Flow and Thermal Field Measurements in a Combustor Simulator Relevant to a Gas Turbine Aeroengine," *ASME J. Eng. Gas Turbines Power*, **127**(2), pp. 257-267.
11. Scrittore, J. J., Thole, K. A., and Burd, S. W., 2005, "Experimental Characterization of Film-Cooling Effectiveness Near Combustor Dilution Holes," GT2005-68704.
12. Shrager, A. C., Thole, K. A., and Mongillo, D., 2018, "Effects of Effusion Cooling Pattern Near the Dilution Hole for a Double-Walled Combustor Liner: Part 2 — Flowfield Measurements." *ASME J. Eng. Gas Turbines Power*, **141**(1), pp. 011023.
13. Ahmed, S., Ramakrishnan, K. R., Ekkad, S., Singh, P., Liberatore, F., Ho, Y., 2020, "Overall Cooling Effectiveness of Effusion Cooled Can Combustor Liner under Reacting and Non-Reacting Conditions," GT2020-15221.
14. Williams, R. P., Dyson, T. E., Bogard, D. G., and Bradshaw, S. D., 2014, "Sensitivity of the Overall Effectiveness to Film Cooling and Internal Cooling on a Turbine Vane Suction Side." *ASME J. Turbomach*., **136**(3), pp. 031006.
15. Mensch, A., and Thole, K. A., 2014, "Overall Effectiveness of a Blade Endwall With Jet Impingement and Film Cooling." *ASME J. Eng. Gas Turbines Power*, **136**(3), pp. 031901.
16. Hollworth, B. R., and L. Dagan, 1980, "Arrays of Impinging Jets with Spent Fluid Removal through Vent Holes on the Target Surface—Part 1: Average Heat Transfer." *ASME J. Eng. Power*, **102**(4), pp. 994-999.
17. Holdeman, J. D., 1993, "Mixing of Multiple Jets with a Confined Subsonic Crossflow." *Progress in Energy and Combustion Science*. **19**(1), pp. 31-70.
18. Moffat, R. J., 1985, "Using Uncertainty Analysis in the Planning of an Experiment." *J. Fluids Eng*., **107**(2), pp. 173–178.
19. Scrittore, J. J., 2008, "Experimental Study of the Effect of Dilution Jets on Film Cooling Flow in a Gas Turbine Combustor," Virginia Polytechnic Institute and State University.